Supplemental Materials.

Supplemental Fig. 1. Lung tumor sizes in radiated and non-radiated groups. Tumor-bearing left lung lobes of mice were photographed using a scale as size reference at day 5 (A) and day 8 (B) after radiation treatment. The H&E staining of the whole lung lobes with the tumors were shown at day 5 (C) and day 8 (D) after radiation treatment.

Supplemental Fig. 2. FLASH^{pr} shows reduced lung tumor burden compared to Control and CONV^{pr}. (A) Representative H&E-stained microscopic images of individual tumors at day 5 post radiation. **(B)** Immunofluorescence staining for mCherry-labelled (Red) tumor cells shows significant reduction of tumor burden at day 5 in FLASH^{pr} group compared to control and CONV^{pr}. Nuclei were counterstained with DAPI (Scale bar 500 μm). **(C)** Representative H&E-stained microscopic images of individual tumors at day 8 post radiation. **(D)** Immunofluorescence staining for mCherry-labelled (Red) tumor cells shows significant reduction of tumor burden at day 8 in FLASH^{pr} group compared to control and CONV^{pr}. Nuclei were counterstained with DAPI (Scale bar 500 μm).

Supplemental Fig. 3. FLASH^{pr} treated tumors present increased number of apoptotic tumor cells. (A) Representative images show distribution of Cleaved Caspase – 3^{+} tumor cells in proton-treated and untreated lung tumors at day 5 and day 8. LLC tumor cells are shown in red (Scale bar 100 μm). **(B)** Number of Cleaved Caspase – 3^{+} tumor cells were counted for each biological replicate and presented as percentage of apoptotic tumor cells per field ± SEM. At least five random fields per group were used to calculate percentage of Cleaved Caspase -3^{+} tumor cells and presented as mean percentage ± SEM. N=3-4 per group. *, $P<0.05$; **, $P<0.01$; ***, $P<0.001$.

Supplemental Fig. 4. FLASH^{pr} reduces the number of macrophages and increases the infiltration of T cells in tumors. (A) Average infiltrated distance of CD8$^+$ cells from tumor edge into the tumor in different proton-irradiated groups at day 5 and day 8 post radiation. Measurement of infiltration distance was performed for individual CD8$^+$ cells and presented as mean ± SEM. *, P<0.05; **, P<0.01; ****, P<0.001. **(B-C)** Representative images show distribution of F4/80$^+$ macrophages (white) in proton-treated and untreated lung tumors at day 5. LLC tumor cells are shown in red and nuclei are counterstained with DAPI (Scale bar 200 μm). Number of mCherry$^+$ tumor cells and F4/80$^+$ macrophages were counted for each biological replicate and presented as the ratio of macrophages to tumor cells per field ± SEM. **(D-E)** Co-localization studies show the distribution of CD8$^+$ cytotoxic T-cells (green) and F4/80$^+$ tumor-associated macrophages (white) among the mCherry-labelled tumor cells (red) in lung tumors of different treatment groups at day 5 (Scale bar 200 μm). Inserts are 20X images showing CD8+ cytotoxic T cells (green) and F4/80$^+$ tumor-associated macrophages (white). Graphs show the ratio of CD8$^+$ T-lymphocytes to F4/80$^+$ macrophages per tumor. Data is representative of complete tumor fields and presented as mean ratio ± SEM. N= 8 per group. *, P<0.05; **, P<0.01; ***, P<0.001.

Supplemental Fig. 5. FLASH^{pr} shows reduced lung tumor burden compared to Control and CONV^{pr}. (A-B) Representative images show CD163$^+$ M2-like macrophages (green) with number of mCherry$^+$ tumor cells after proton radiation at day 5 and day 8. Nuclei were counterstained with DAPI (Magnification 200x). Graphs are representative of corelation of numbers of CD163$^+$ cells and tumor cells in random fields distributed across groups. **(C-D)** Representative images show the distribution of iNOS$^+$ M1-like macrophages (green) in tumors after FLASH^{pr} and CONV^{pr} radiation. Tissue sections were counterstained with DAPI (Magnification 200x). Graph shows

correlation of iNOS$^+$ cells and tumor cells in random fields distributed across groups. N = 3-8 mice per group. *, P<0.05; **, P<0.01; ***, P<0.001.

Supplemental Fig. 6. (A) Co-localization studies demonstrate the decrease in the number of CD163$^+$ cells (red) and the increase in the number of CD3$^+$ T-lymphocytes (green) in the irradiated lung tumors compared to untreated tumors. Representative images of CD3$^+$ T-cells and CD163$^+$ cells at day 5 (Scale bar 100 μm). **(B)** Co-localization studies demonstrate the increase in the number of iNOS$^+$ cells (red) and the increase in the number of CD3$^+$ T-lymphocytes (green) in the radiation-treated lung tumors compared to untreated tumors. Representative images of CD3$^+$ T-cells and iNOS$^+$ cells distribution at day 5 (Scale bar 100 μm).

Supplemental Fig. 7. FLASH^{pr} inhibits expression of checkpoint inhibitors PD-1 and PD-L1. (A-B) Co-localization studies show the expression of PD-1 (red) among CD3$^+$ T-lymphocytes (green) in lung tumors of different treatment groups at day 5. Nuclei were counterstained with DAPI (Scale bar 50 μm). At least five random fields per group were used to calculate percentage of PD-1$^+$ T-lymphocytes and presented as mean percentage ± SEM. N=3 per group. *, P<0.05; **, P<0.01; ***, P<0.001. **(C-D)** Co-localization studies show the expression of PD-L1 (green) among lung tumor cells (red) in different treatment groups at day 5. Nuclei were counterstained with DAPI (Scale bar 50 μm). At least five random fields per group were used to calculate percentage of PD-L1$^+$ tumor cells and presented as mean ratio ± SEM. N=3 per group. *, P<0.05; **, P<0.01; ***, P<0.001.

Supplemental Fig.1

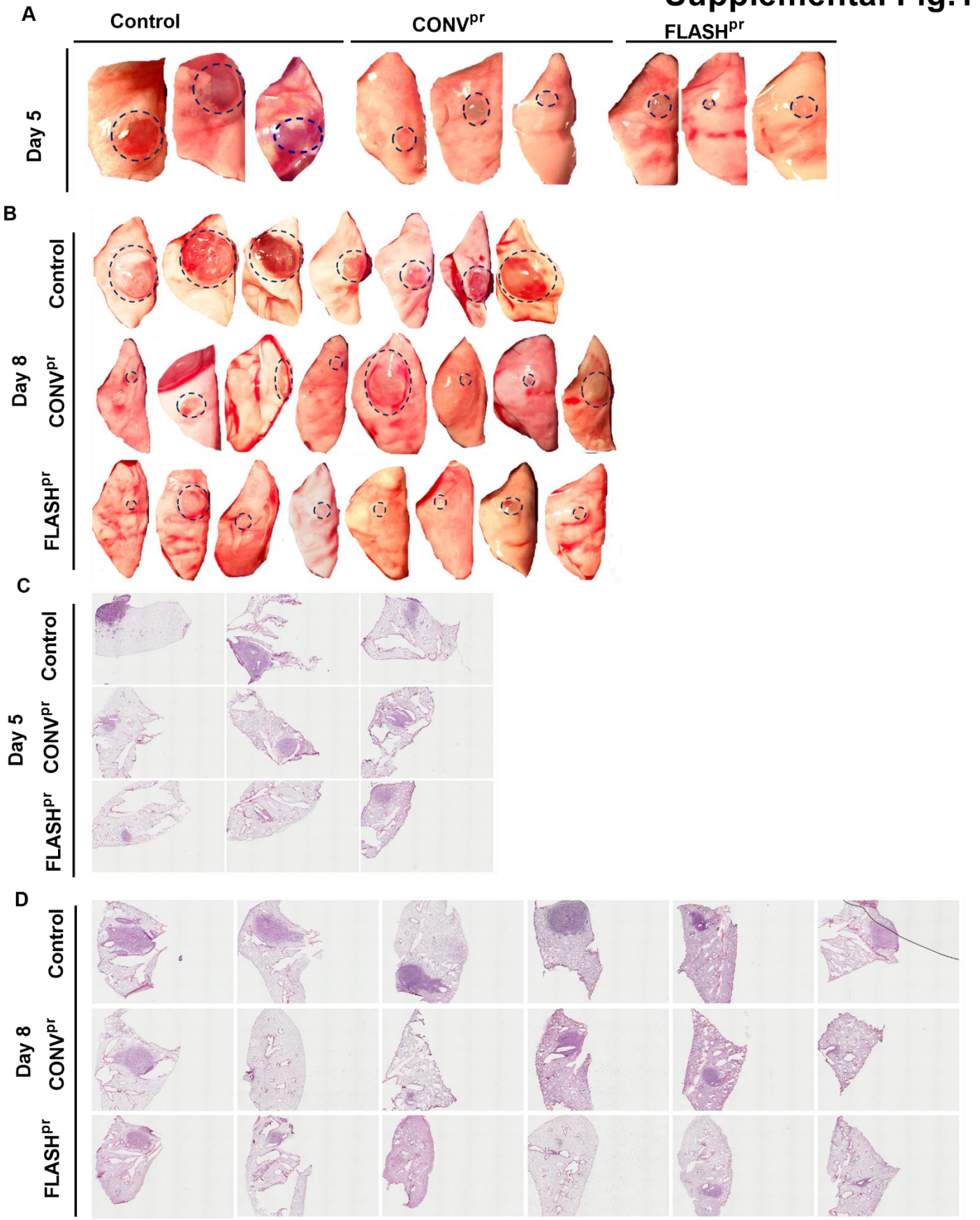

Supplemental Fig.2

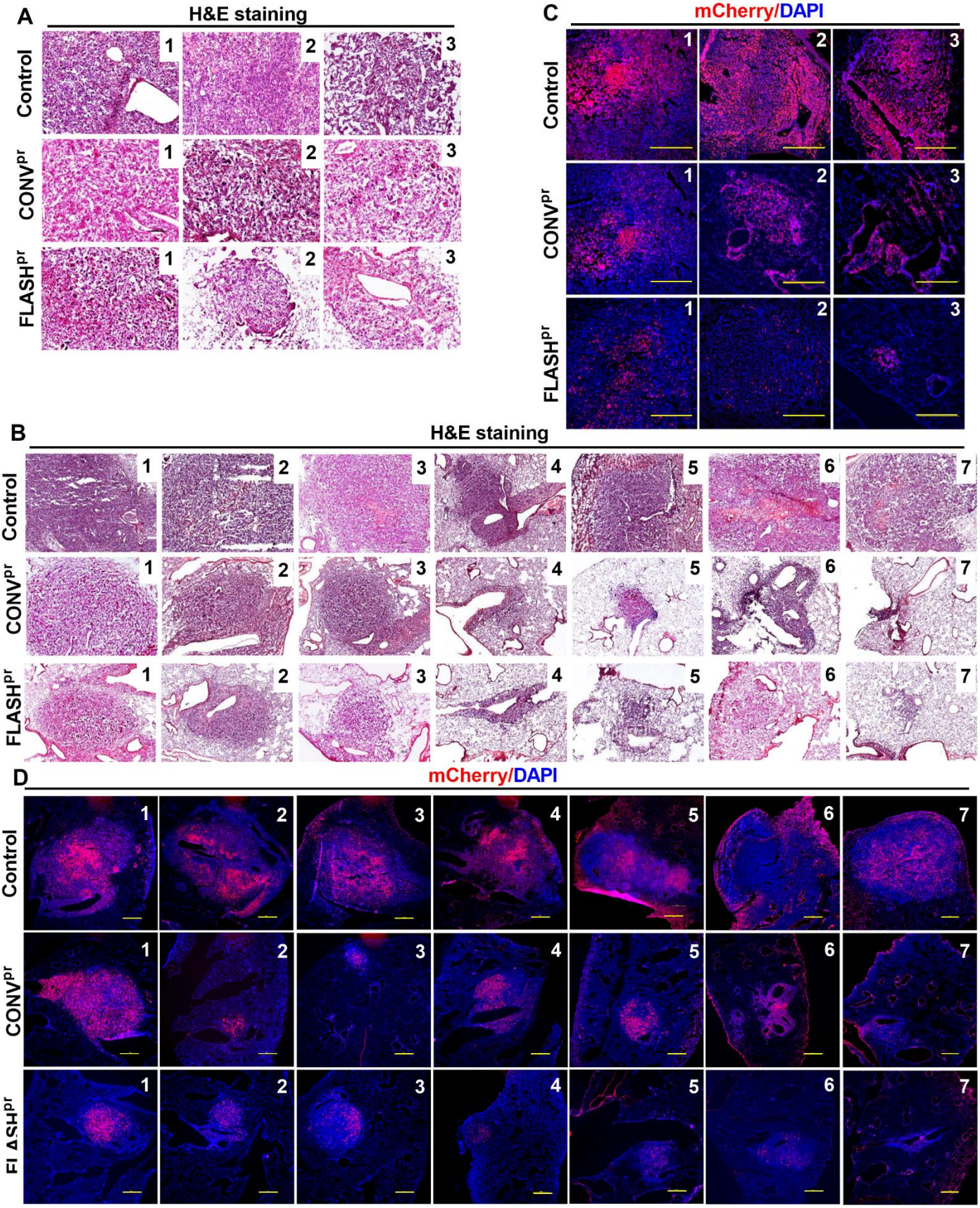

Supplemental Fig.3

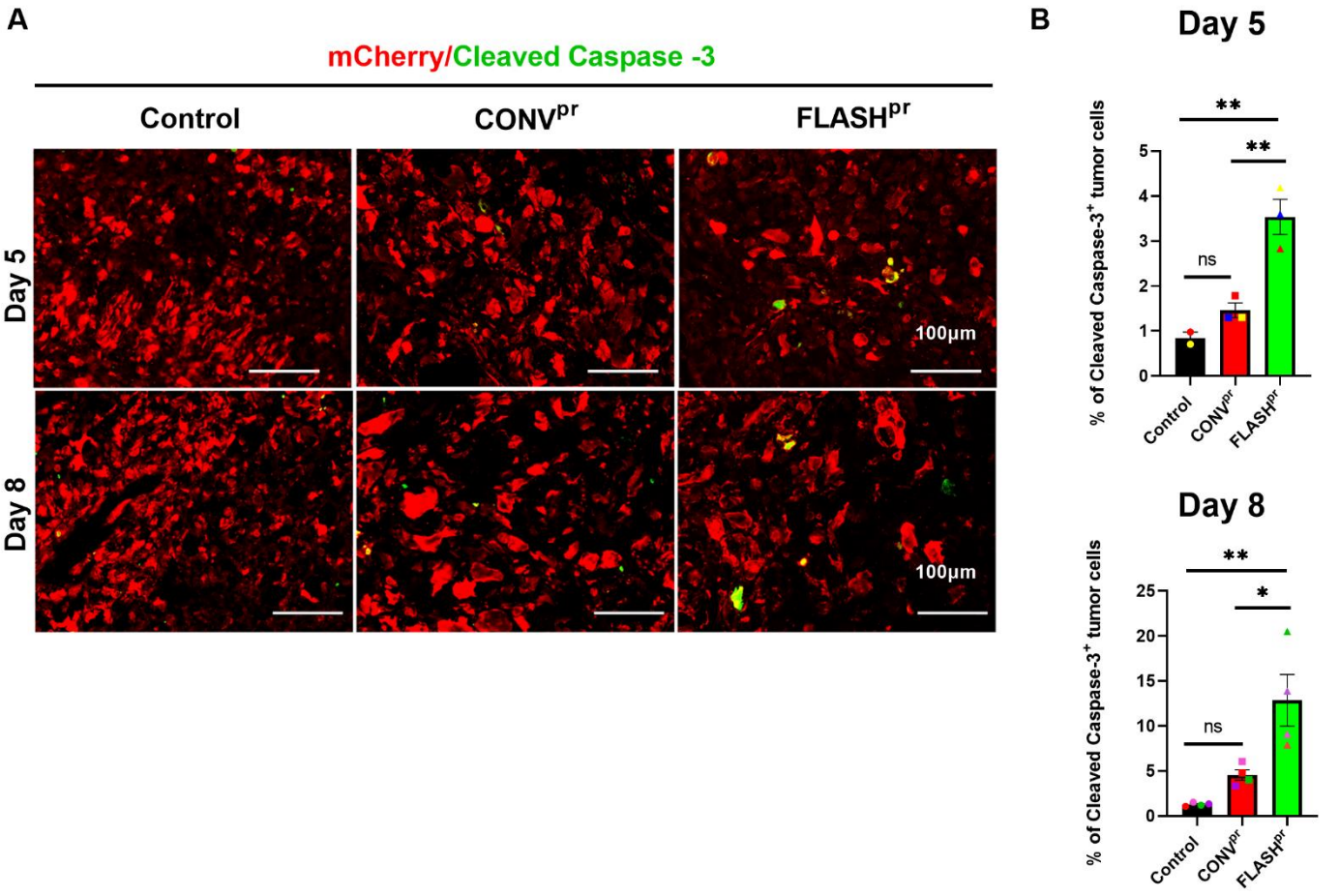

Supplemental Fig. 4

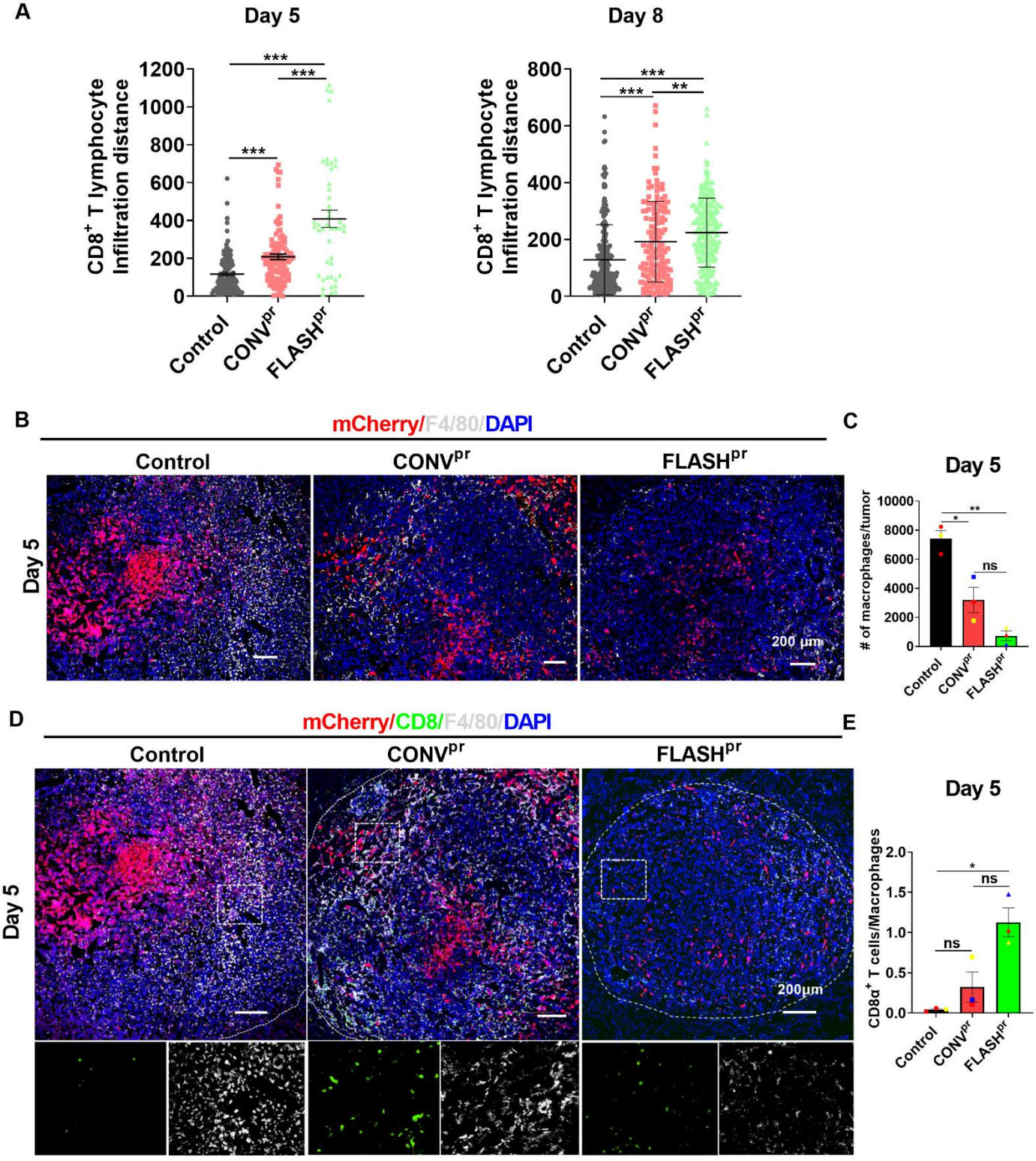

Supplemental Fig. 5

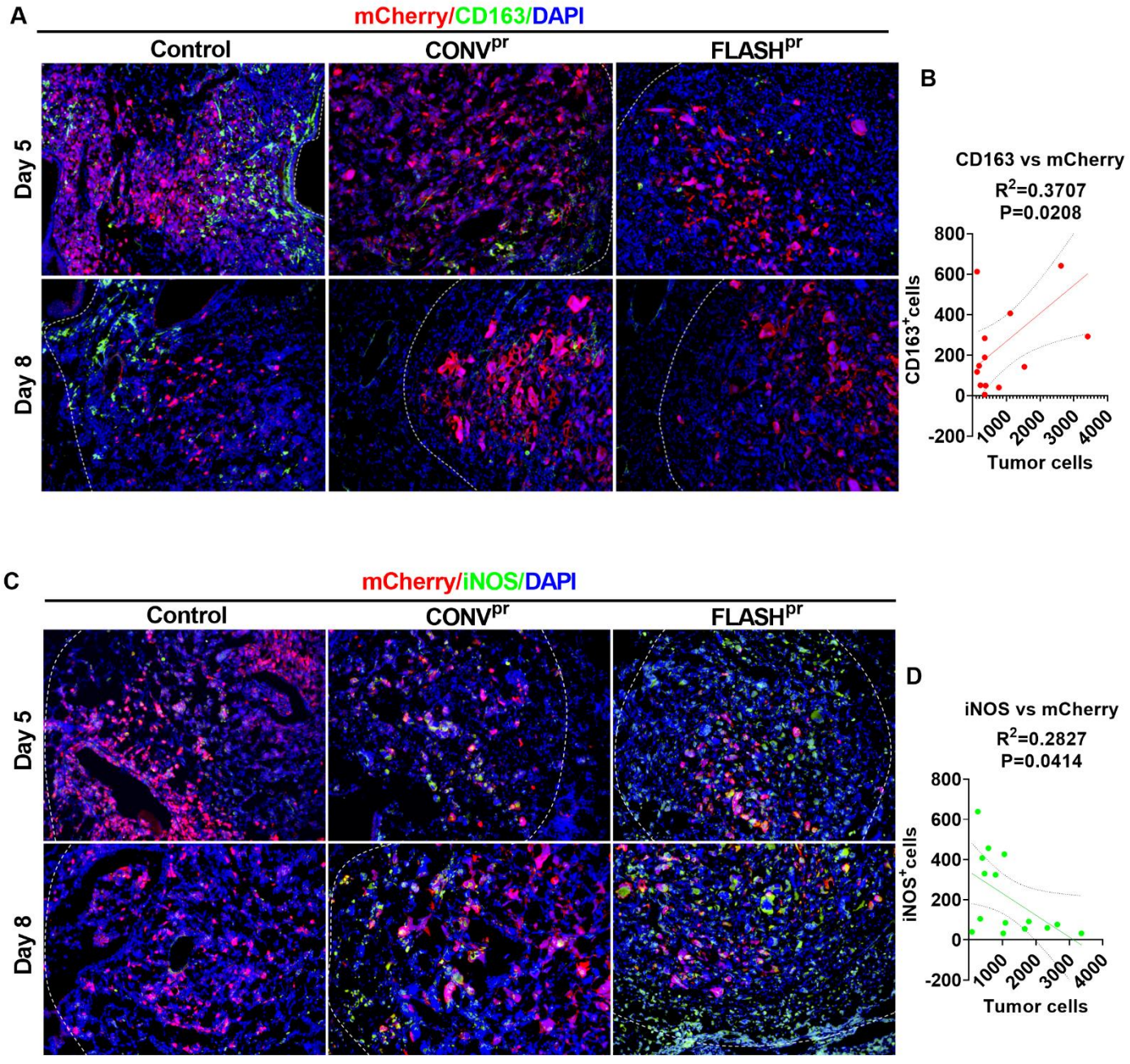

Supplemental Fig. 6

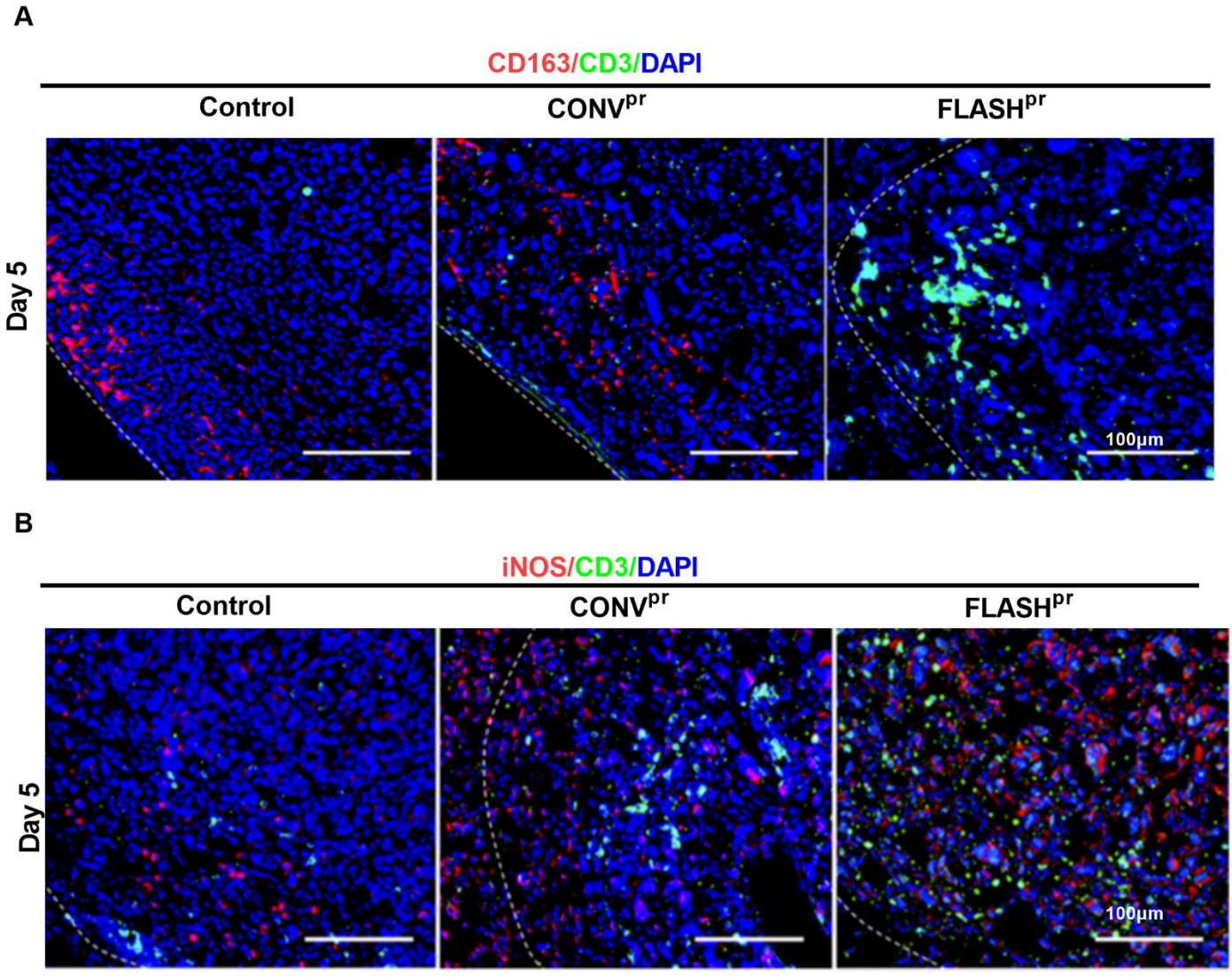

Supplemental Fig. 7